Multiphase fringe analysis with unknown phase shifts

Gordon D. Lassahn
Jeffrey K. Lassahn
Paul L. Taylor
Vance A. Deason
EG&G Idaho, Inc.
P.O. Box 1625
Idaho Falls, Idaho 83415-2211

Abstract. We present methods for determining the phase shifts in multiphase fringe analysis from the fringe image data itself, thus eliminating the requirement for prior knowledge or accurate control of the phase shifts. We also discuss methods for calculating the folded (wrapped) and unfolded phases, and quote the accuracy of the fringe analysis method for an example in which the correct result is known.

Subject terms: algorithms.

Optical Engineering 33(6), 2039–2044 (June 1994).

1 Introduction

Fringe analysis is a measurement tool in which images of optical interference fringes are used to indicate spatial variations of some physical parameter such as displacement or gas density. In a typical application of diffraction moire fringe analysis, for example, two coherent light beams illuminate a diffraction grating and two diffracted beams interfere with each other to produce a fringe pattern, the details of which depend on distortions either of the grating or of the wavefronts of the incident light beams. In multiphase fringe analysis measurements, several images of interference fringes are recorded from the same experiment, with each successive image having a different amount of phase shift added to one of the incident light beams. The advantages of having multiple, phase-shifted interference fringe images are two: resolution of certain ambiguities in data interpretation and less sensitivity to noise in the data.

The older methods of interpreting multiphase fringe data require that the phase shifts for the several fringe images are known or are unknown but all the same. However, multiphase fringe analysis can be done with phase shifts of arbitrary values (except for certain degenerate combinations of values).[1] It is generally conceded that, even though the phase shift values can be arbitrary, they must be known accurately. This means that the phase shift values must be set accurately to some preselected values, which requires sophisticated phase-shifting hardware, or that simpler phase-shifting hardware can be used if there is some method for accurately measuring the phase shifts. Lai and Yatagai[2] report a method of recording extra fringe data that allows easy determination of the phase shifts. Okada, Sato, and Tsujiuchi[3] report an iterative method for extracting the phase shift values from the fringe image data, assuming that there is available some reasonable first guess at the phase shift values. The results they discuss use a large number (32) of phase-shifted fringe images and random errors in the first-guess phase shift values; there is some question about whether their method can work with a small number (3 to 5) of fringe images or with first-guess values that are not random (all too large, for example). Farrell and Player[4] report a method of extracting the phase shift values from the fringe images using a Lissajous figure calculation, which appears to be satisfactory.

This paper discusses two alternative methods for eliminating this requirement for uniform or known phase shifts in the analysis of multiphase interference fringe data. One method requires the recording of two extra images along with the fringe image data, and the other requires no extra data but does require a little operator interaction.

2 Statement of the Problem

We are given a set of K images of fringe patterns, each produced by the interference of two coherent light beams. The phase difference between the two light beams is different for the K different images; let Δ_k be the phase shift added to one of the incident light beams when recording image k, $k = 2, 3, \ldots K$, relative to the phase for image 1. Then the intensity at the pixel at column i and row j in image k can be written as

$$I_k(i,j) = A(i,j) + B(i,j)\ \cos[\Phi(i,j) + \Delta_k] + \text{error}\ , \qquad (1)$$

where $\Phi(i,j)$ is the phase difference between the two beams at pixel i,j for image 1. This Φ is the quantity we wish to determine. The intensities I are measured in the experiment;

Paper 32053 received May 29, 1993; revised manuscript received Oct. 18, 1993; accepted for publication Nov. 14, 1993.

they are simply the brightnesses of the pixels in the given images of the fringe patterns. Here $A(i,j)$ and $B(i,j)$ describe the intensities of the two incident beams and the fringe contrast; A and B are assumed to be smooth, slowly varying functions of i and j. The error is assumed random, unknown, and small.

3 Calculation of the Folded Phase

For any pixel, we can express the phase Φ as

$$\Phi(i,j) = \Psi(i,j) + 2\pi N(i,j) \ , \tag{2}$$

where N is some integer and $0 \leq \Psi < 2\pi$. This Ψ is called the folded or wrapped phase. We can calculate Ψ if we know Δ_k and assume that A and B are independent of k, for any given i,j. For each pixel, we rewrite Eq. (1) (not bothering to write the row and column indexes i and j) as

$$I_k = P1 + P2 \ \cos(\Delta_k) - P3 \ \sin(\Delta_k) + \text{error} \ , \tag{3}$$

where $P1 = A$, $P2 = B \cos(\Psi)$, and $P3 = B \sin(\Psi)$. This represents K equations in the three unknowns $P1$, $P2$, and $P3$. If K is greater than 3, we can calculate the three unknowns using a linear least-squares calculation. This approach has been used by others.[1] The coefficient matrix for the least squares calculation is the same for all pixels; therefore, we can solve the set of least-squares equations once and for all, rather than solving separately for each pixel. Then $P2$ and $P3$ can be found for each pixel by calculating a few simple sums, and then the phase at that pixel can be calculated by

$$\Psi = \text{atan2}(P3, P2) \ , \tag{4}$$

where atan2 is a function that calculates an angle when it is given the opposite side and the adjacent side of a right triangle. We also calculate

$$B = \text{sqrt}(P3*P3 + P2*P2) \ , \tag{5}$$

as an indicator of the validity of the phase calculation for this pixel. If B is too small, either the fringes are of very low contrast or something else has gone wrong with the phase calculation. In this case, the pixel is declared invalid and no phase is calculated for that pixel. Note that we do not need to calculate the value of $P1$, although we must allow it to be an adjustable parameter to achieve a meaningful fit of Eq. (3) to the data.

4 Unfolding the Phase

Unfolding or unwrapping the phase is done by a procedure that is in most ways quite standard, adding multiples of 2π to the folded phase at each pixel to make that pixel's unfolded phase close to that of its neighboring pixels. The present procedure uses an adaptive criterion to decide whether each pixel fits with its neighbors well enough to allow unfolding. If none of the still-folded pixels fits well enough to be unfolded, the criterion is relaxed to some maximally tolerant value. When some pixels can be unfolded, the criterion is gradually made more stringent. This has the effect of unfolding the best fitting pixels first and delaying the questionable pixels, which tends to avoid making unfolding errors early in the process and allowing those errors to affect later unfolding.

5 Calculating Phase Shifts between Fringe Images

The procedure described earlier for calculating the folded phase Ψ requires knowledge of Δ_k, the phase difference between the two light beams for fringe pattern k relative to that for fringe pattern 1. We describe two alternative methods for determining Δ_k, referred to as the line-drawing method and the beam-shuttering method.

6 Line-Drawing Method

To estimate the Δ_k values, we first specify a straight line segment on the images such that the line spans approximately one full fringe cycle in a region where the phase Φ is approximately a linear function of position, where the fringe that is spanned is fairly broad, and where there is not too much noise in the raw data. In simple terms, the intensity versus position along this line is fitted with a cosine function to determine a phase Δ_k for each of the fringe images. This process is explained in more detail as follows.

Let s be the position along this line, and let Φ along this line be specified by a polynomial approximation:

$$\Phi = \Phi(s=0) + \phi(s) \ , \tag{6}$$

where $\Phi(s=0)$ is simply the phase Φ at one end of the line and

$$\phi(s) = \alpha_1 s + \alpha_2 s^2 + \cdots + \alpha_m s^m + \cdots + \alpha_M s^M, \ m = 1,2,\ldots,M. \tag{7}$$

The number of terms M is specified beforehand to be some low value, like 2. Allowing M to be greater than 1 accounts for nonlinearity in the phase versus position relationship. The α_m are to be determined. As a first estimate, α_1 is simply 2π divided by the line length, and the other α_m are 0. (These α values would be exactly correct for the ideal situation of linear phase versus position with no noise.) For fringe image k, the intensity along the selected line can be written as

$$I_k(s) = A + B \ \cos[\Phi(s) + \Delta_k] = A + B \ \cos[\phi(s) + \Lambda_k] \ , \tag{8}$$

where $\Lambda_k = \Delta_k + \Phi(s=0)$. We assume that the number of pixels along the specified line segment is greater than $K+M$. Then we can determine the Λ_k and the α_m by a nonlinear least-squares fitting procedure. This requires first estimates for the α_m, which we already have, and for the Λ_k, which are obtained as follows:

$$E = \int I_k \ \cos[\phi(s)]\alpha_1 ds = \int I_k \ \cos(\phi) \ d\phi = B \ \cos(\Lambda_k)/2 \ , \tag{9}$$

and

$$F = \int I_k \ \sin[\phi(s)]\alpha_1 ds = \int I_k \sin(\phi) \ d\phi = -B \ \sin(\Lambda_k)/2 \ , \tag{10}$$

assuming that $\phi(s) = \alpha_1 s$ and the line segment is one cycle long. The integrals F and E can of course be approximated

by sums over the pixels in the line segment, which then allows the first estimate:

$$\Lambda_k = -\text{atan2}(F, E) \ . \tag{11}$$

After these first estimates are obtained, better values for the Λ_k and the α_m can be obtained by the usual iterative, nonlinear least-squares fitting procedure. Finally, we can do the trivial (and not really necessary) transformation

$$\Delta_k = \Lambda_k - \Lambda_1 \ . \tag{12}$$

This is the desired result.

7 Beam-Shuttering Method

There is a second method for calculating the Δ_k, which does not require any operator intervention (drawing a line spanning one fringe). However, it does require that we record two additional images, one with the first incident beam blocked and the other with the second incident beam blocked. Thus, these two images represent simply the intensities of the two separate incident beams. These two additional images allow us to, in effect, eliminate the unknowns A and B from Eq. (1). We must still cope with the ambiguity in the inverse cosine function; this is done by sampling the images at a number of different pixels and looking for consistent choices about which branch of the inverse cosine function to use. Taking samples at several pixels also tends to average out whatever noise may be present. Details of this process are as follows.

For convenience, we will refer to these two shuttered-beam images as L and R. For any pixel, we can use the L and R image intensity values to calculate a "normalized intensity" for that pixel in the k'th fringe image:

$$J_k = (I_k - L - R)/[2(LR)^{1/2}] \ . \tag{13}$$

Except for the effects of noise or measurement error, this normalized intensity is equal to the cosine of the total phase for that pixel in fringe image k:

$$\cos(\Phi + \Delta_k) = J_k \ . \tag{14}$$

In this system, we assume that the phase shift between two successive fringe images is never greater than π. With this restriction in mind, to calculate the phase difference between two successive fringe images—say $\Delta_2 - \Delta_1$, for example—we look at the same pixel in the two normalized fringe images. If either of these two normalized intensities has an absolute value close to 1.0 (say, greater than 0.9), we do not use this pixel to estimate the phase difference, because such values give excessive sensitivity to small errors in the data. If the absolute values of the normalized intensities are acceptable far from 1.0, then the absolute value of the phase difference is given by one of two calculations:

$$D_1 = ABS[\arccos(J_2) - \arccos(J_1)] \ , \tag{15}$$

and either of

$$D_2 = ABS[\arccos(J_2) + \arccos(J_1)] \tag{16}$$

or

$$D_2 = 2\pi - ABS[\arccos(J_2) + \arccos(J_1)] \ , \tag{17}$$

depending on which D_2 value is less than π. There is no way to tell from this pixel alone which of D_1 or D_2 is the correct phase difference. We enter both of these values in a list of pairs of possible values for $\Delta_2 - \Delta_1$. We also make a rough estimate of the uncertainty of these two values, based on the assumption of equal uncertainties for all normalized intensity values, and enter that uncertainty value into a list. We then repeat this process for perhaps 100 or a few hundred other pixels, thus generating a list of pairs of values with perhaps 100 entries and a list of uncertainty values.

After the list is made, we compare each entry in the list with every other entry in the list of pairs of $\Delta_2 - \Delta_1$ values. Ideally, each entry should contain one correct value and one incorrect value, so one value from one entry should be equal to one value from the other entry and the other two values should be different (although perhaps not much different). Therefore, in the comparison, if we find two approximately equal values (within 0.1 rad) and two other values that are significantly different (by more than 0.2 rad), we consider the two nearly equal values to be reasonable estimates of the correct $\Delta_2 - \Delta_1$ value and we include these two values in a weighted average that will give a (hopefully) good estimate of the correct value. The weighting coefficient for each value included in the average is the inverse of the square of the uncertainty of that value.

8 Accuracy

To check these procedures, we synthesized a set of five fringe images and two shuttered images. The incident beam phase differences Δ_k for the five fringe images are 0 (by definition for the first fringe image), 30, 90, 180, and 300 deg. This synthetic data set includes no noise except for the truncation error associated with representing the intensities with 8-bit integers. Both the average intensity and the contrast are slowly varying functions of position. Figure 1 shows the

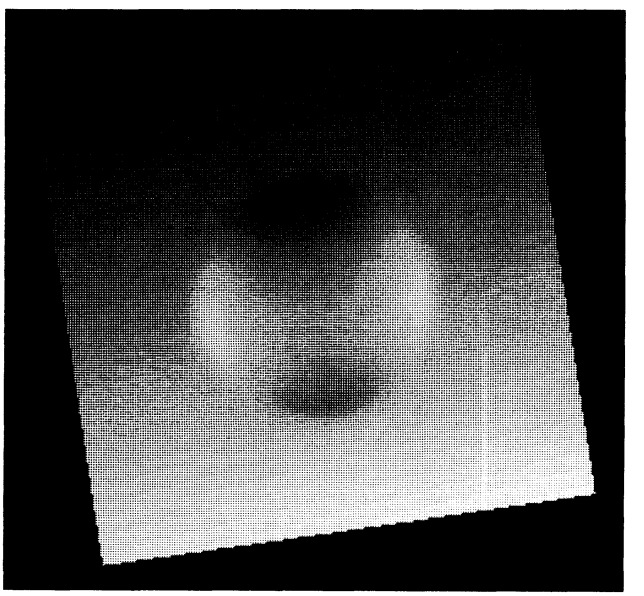

Fig. 1 Phase map for synthetic data set. Phase is represented as brightness in this figure. The total phase range is about four fringes (8π rad).

phase, represented as brightness in this figure. The total range of the phase values is about four fringes. The first fringe image is shown in Fig. 2. This data set includes local extrema (closed loop fringes) and a saddle point in the phase map, which present no special difficulty to the algorithms presented here.

We list here the results of one analysis using the shuttered images, which should be the same for repeated analyses of the same data set, and three analyses using the line-drawing method without the shuttered images, which may give different (hopefully not much different) results depending on where the operator draws the line. The results of these four analyses are listed in Table 1. The column headed "S.B." gives the results for the first analysis, which uses the shuttered images, and the next three columns, headed "L.D.1," "L.D.2," and "L.D.3," give the results for the three analyses using the line-drawing method. The column headed "IDEAL" gives the correct or ideal values.

Table 1 lists the calculated phase shifts Δ_k for the four analyses, in degrees. The first analysis, which used the shuttered images, is a little more accurate in this respect than the other three, which used the line-drawing method.

Table 1 also lists five indicators of the error in the calculated phase for each of the four analyses, obtained by direct comparison of the fringe analysis program's output with the known correct phases for this synthetic data set. In this comparison, any overall difference that is a multiple of 2π is ignored. Perhaps the most useful error indicator is the standard deviation of the distribution of the errors in the calculated phase. In these calculations, the results of the phase analysis program were output in the form of integer values with a truncation error of $\pm 1/512$ fringe, so the minimum expected standard deviation is 0.0011 fringe even if there are no calculation errors and no noise in the input data. The average error is usually not significant in practical applications. The minimum and maximum error values are, of course, affected by the average error value; the error range, the difference between the maximum error and the minimum error, is usually a more meaningful error indicator than the minimum or maximum values themselves.

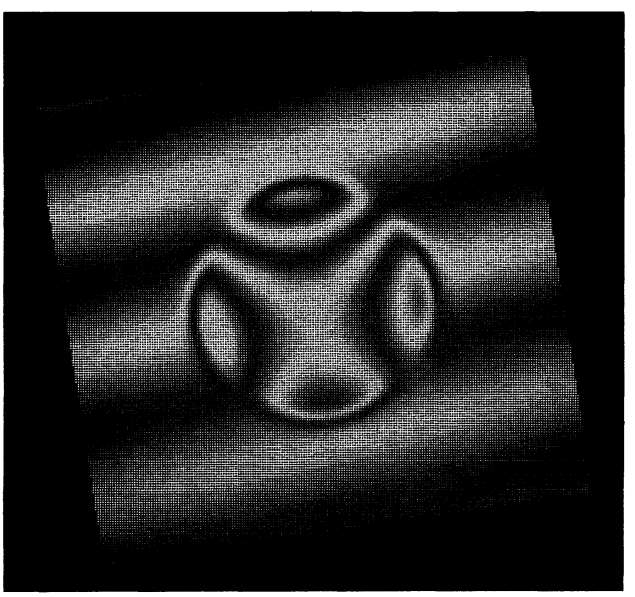

Fig. 2 The first fringe image of the synthetic data set.

Table 1 Fringe analysis results with no noise.

S.B.	L.D.1	L.D.2	L.D.3	IDEAL	
29.97	30.19	30.20	32.08	30.00	PHASE SHIFT Δ_2 [degrees]
90.19	93.40	92.12	97.30	90.00	PHASE SHIFT Δ_3 [degrees]
179.21	181.06	181.22	189.10	180.00	PHASE SHIFT Δ_4 [degrees]
299.04	299.17	302.79	302.07	300.00	PHASE SHIFT Δ_5 [degrees]
0.596	0.647	0.976	0.556	0.406	STANDARD DEVIATION [degrees]
0.0017	0.0018	0.0027	0.0015	0.0011	STANDARD DEVIATION [fringes]
-1.018	-2.263	-2.880	-6.101	0.0000	AVERAGE ERROR [degrees]
-.0028	-.0063	-.0080	-.0169	0.0000	AVERAGE ERROR [fringes]
-3.162	-4.588	-5.693	-8.007	-0.703	MINIMUM ERROR [degrees]
-.0088	-.0127	-.0158	-.0222	-.0020	MINIMUM ERROR [fringes]
0.993	-0.445	-0.560	-3.864	0.703	MAXIMUM ERROR [degrees]
0.0028	-.0012	-.0016	-.0107	0.0020	MAXIMUM ERROR [fringes]
4.155	4.143	5.133	4.143	1.406	ERROR RANGE [degrees]
0.0116	0.0115	0.0142	0.0115	0.0039	ERROR RANGE [fringes]

It is interesting to note that errors of several degrees in the phase shift values do not seem to cause a significant increase in the errors in the final calculated phases at the individual pixels. In the worst case in Table 1, the error standard deviation is only 0.0027 fringe and the error range is only 0.0142 fringe.

The tests represented in Table 1 are for data with no noise (except for roundoff error). To evaluate these fringe analysis procedures with more realistic data, we added noise to the fringe images used in the previous tests. The noise was approximately Gaussian distributed, with root-mean-square magnitudes (standard deviations) of 2, 5, 10, and 20 intensity units. The full range of intensity values in the fringe images is 0 through 255, and the average intensity and the fringe amplitude [A and B in Eq. (1)] are 100 and 50 at the center of the fringe pattern (they vary a little with position). In some cases, particularly with the larger noise levels, the added noise caused the itensities of some pixels to extend beyond the acceptable range of 0 to 255; in these cases, the out-of-range intensity value was simply truncated to force it to be within range.

The noisy data sets were analyzed in the same way as the no-noise data, with one analysis (S.B.) using the shuttered images and three analyses (L.D.1, L.D.2, and L.D.3) using the line-drawing method without the shuttered images. The results are listed in Tables 2 through 5. In these tables, the standard deviation value in the IDEAL column is a theoretical estimate of the root-mean-square error in the individual pixel phase values, resulting from the noise in the fringe images, assuming no error in the overall phase shifts Δ_k. With the larger noise levels, a significant fraction of the pixels was declared "bad" by the fringe analysis program. They could not be analyzed because the fringe contrast appeared too low or because the noisy intensity values were in some way not compatible with the expected form. Tables 4 and 5 indicate

Table 2 Fringe analysis results with noise = 2.

S.B.	L.D.1	L.D.2	L.D.3	IDEAL	
34.77	32.07	28.75	31.93	30.00	PHASE SHIFT Δ_2 [degrees]
101.67	93.68	88.89	92.97	90.00	PHASE SHIFT Δ_3 [degrees]
192.19	183.88	179.88	179.07	180.00	PHASE SHIFT Δ_4 [degrees]
300.33	296.85	301.29	293.33	300.00	PHASE SHIFT Δ_5 [degrees]
3.796	3.823	3.828	3.843	1.593	STANDARD DEVIATION [degrees]
0.0105	0.0106	0.0106	0.0107	0.0044	STANDARD DEVIATION [fringes]
-10.75	-5.634	-4.129	-3.429	0.0000	AVERAGE ERROR [degrees]
-.0299	-.0157	-.0115	-.0095	0.0000	AVERAGE ERROR [fringes]

Table 3 Fringe analysis results with noise = 5.

S.B.	L.D.1	L.D.2	L.D.3	IDEAL	
37.97	29.16	27.79	30.54	30.00	PHASE SHIFT Δ_2 [degrees]
111.85	86.00	89.24	90.02	90.00	PHASE SHIFT Δ_3 [degrees]
199.56	178.88	187.37	181.34	180.00	PHASE SHIFT Δ_4 [degrees]
302.87	299.85	305.21	303.72	300.00	PHASE SHIFT Δ_5 [degrees]
5.358	5.357	5.388	5.345	3.878	STANDARD DEVIATION [degrees]
0.0149	0.0149	0.0150	0.0148	0.0108	STANDARD DEVIATION [fringes]
-15.99	-2.930	-6.778	-5.590	0.0000	AVERAGE ERROR [degrees]
-.0444	-.0081	-.0188	-.0155	0.0000	AVERAGE ERROR [fringes]

Table 4 Fringe analysis results with noise = 10.

S.B.	L.D.1	L.D.2	L.D.3	IDEAL	
40.13	35.34	28.94	29.96	30.00	PHASE SHIFT Δ_2 [degrees]
108.81	96.68	84.31	85.52	90.00	PHASE SHIFT Δ_3 [degrees]
199.01	180.21	181.52	178.64	180.00	PHASE SHIFT Δ_4 [degrees]
296.49	295.09	306.12	298.23	300.00	PHASE SHIFT Δ_5 [degrees]
8.950	8.851	8.934	8.865	7.715	STANDARD DEVIATION [degrees]
0.0249	0.0246	0.0248	0.0246	0.0214	STANDARD DEVIATION [fringes]
-13.90	-5.534	-4.618	-2.525	0.0000	AVERAGE ERROR [degrees]
-.0386	-.0154	-.0128	-.0070	0.0000	AVERAGE ERROR [fringes]
0.48	0.49	0.54	0.52	0.00	% BAD PIXELS

the percentage of pixels declared bad for noise levels of 10 and 20. For lower noise levels, the percentage of bad pixels was less than 0.01%.

Tables 2 through 5 indicate that the calculation of phase shifts using the shuttered images is much more susceptible to noise than is the line-drawing method, which shows surprisingly little sensitivity to the noise levels tested here. As with the no-noise test, we see that relatively large errors in the calculation of the phase shift values do not seem to significantly increase the noise in the final result, the phases

Table 5 Fringe analysis results with noise = 20.

S.B.	L.D.1	L.D.2	L.D.3	IDEAL	
51.31	33.74	27.23	30.36	30.00	PHASE SHIFT Δ_2 [degrees]
115.27	87.51	91.53	90.93	90.00	PHASE SHIFT Δ_3 [degrees]
203.44	181.52	171.45	181.37	180.00	PHASE SHIFT Δ_4 [degrees]
299.42	305.78	295.42	295.90	300.00	PHASE SHIFT Δ_5 [degrees]
15.87	15.85	15.92	15.77	15.43	STANDARD DEVIATION [degrees]
0.0441	0.0440	0.0442	0.0438	0.0429	STANDARD DEVIATION [fringes]
-18.97	-6.050	-1.101	-3.891	0.0000	AVERAGE ERROR [degrees]
-.0527	-.0168	-.0031	-.0108	0.0000	AVERAGE ERROR [fringes]
19.63	18.87	19.03	18.76	0.00	% BAD PIXELS

calculated for the individual pixels. That is, for each of the tables, the first column compared to the next three columns indicates relatively large errors for the overall phase shifts (phase shift Δ_k) but comparable root-mean-square errors for the individual pixel phases (standard deviation). This conclusion is further supported by the observation that the actual standard deviation values, including the effects of the errors in the overall phase shifts Δ_k, are not much larger than the ideal standard deviation values predicted with the assumption of no errors in the overall phase shifts Δ_k. For example, in Table 5, the Δ_k values in the first column have errors as large as 21, 25, and 23 degs, which seem quite large; but, the root-mean-square error in the individual pixel phases (standard deviation) for this case is 0.0441 fringes, comparable with the standard deviation values in the L.D. columns, which have smaller Δ_k errors, and only slightly larger than the estimated ideal standard deviation value of 0.0429 fringes.

9 Conclusions

Phase-shifted fringe analysis can be a highly automated process with small errors in the final results. The system used here requires, as a minimum, that the operator choose a starting point for the unfolding process; in a more interactive option, the operator must also mark a line spanning one fringe in a low-noise region of the image. With synthetic fringe image data, this system gives phase calculation errors with a standard deviation no worse than 0.0027 for input data with no noise, and it gives approximately the theoretically predicted phase errors for noisy data. This analysis can be done without any stringent requirement for phase shift values, such as particular values, regularly spaced values, or accurately controlled values.

Acknowledgment

This work was supported by the U.S. Department of Energy (DOE) under DOE Field Office, Idaho, Contract No. DE-AC07-76ID01570.

References

1. J. E. Greivenkamp, "Generalized data reduction for heterodyne interferometry," *Opt. Eng.* **23**(4), 350–352 (1984).
2. G. Lai and T. Yatagai, "Generalized phase-shifting interferometry," *J. Opt. Soc. Am. A* **8**(5), 822–827 (1991).

3. K. Okada, A. Sato, and J. Tsujiuchi, "Simultaneous calculation of phase distribution and scanning phase shift in phase shifting interferometry," *Opt. Commun.* **84**(3,4) 118–124 (1991).
4. C. T. Farrell and M. A. Player, "Phase step measurement and variable step algorithms in phase-shifting interferometry," *Measurement Sci. Technol.* **3,** 953–958 (1992).

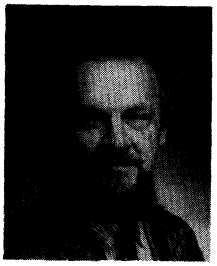

Gordon D. Lassahn has BS and PhD degrees in physics from Iowa State University. He has worked in several areas of data analysis and interpretation and uncertainty estimation.

Jeffrey K. Lassahn is an undergraduate student in physics and mathematics at the University of Oregon. He developed some of the fringe analysis algorithms during a summer job at the Idaho National Engineering Laboratory.

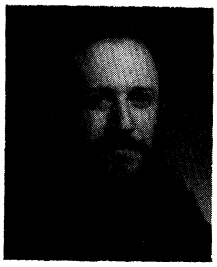

Paul L. Taylor has his MS in welding engineering from the Ohio State University. His work experience has involved development of sensors and controls for welding and other processes using personal computers for image processing, data acquisition/processing, and data display.

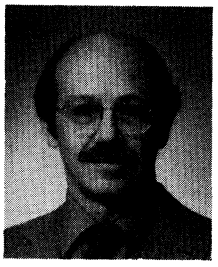

Vance A. Deason has a BS in physics from the University of Colorado. He has been involved for many years in the design of interferometric systems.